Feasible Region for a Countercurrent Cascade of Vapor-Liquid CSTRs

Sagar B. Gadewar, Michael F. Malone, and Michael F. Doherty
Dept. of Chemical Engineering, University of Massachusetts, Amherst, MA 01003

The attainable region approach for reaction-mixing systems was applied to systems with simultaneous reaction and separation. A model developed for a countercurrent cascade of two-phase CSTRs can be considered as a surrogate for the stripping or rectifying sections of a reactive distillation column. An overall composition vector defined satisfies the same geometric properties as the reaction vector. The necessary conditions for the reaction-mixing attainable region were applied to the cascade of two-phase CSTRs. This article focuses only on the countercurrent cascade of two-phase CSTRs; therefore, the region identified is a feasible region, which is a subset of the attainable region for reaction-separation systems. For consecutive reactions, the boundary of the feasible region is given by the trajectory for a cocurrent cascade of two-phase CSTRs. The overall composition vector for the cocurrent cascade of two-phase CSTRs is tangent to the trajectory. For single reversible reactions, the attainable region for single-phase reactors is significantly expanded by using a countercurrent cascade of vapor-liquid CSTRs. Two examples used are transalkylation of toluene and the synthesis of isopropyl acetate.

Introduction

Reactor network synthesis studies determine reactor types and sizes, and their arrangement in a network. The reaction system in a flowsheet dictates the downstream processes (such as separation and waste treatment) and strongly influences the flowsheet structure and economics. An early approach found optimal temperature profiles and residence-time distributions for reactors (Aris 1960a,b,c, 1961) as in dynamic programming for a fixed reactor system and sequential processes. Another approach is superstructure optimization, which involves specification of a superstructure network of reactors, and optimization selects a subnetwork. The reactor network obtained, however, depends on the types of reactors selected and the initial superstructure chosen. A selection of possibilities include the following. Jackson (1968) published a reactor superstructure consisting of PFRs connected by sidestreams. Chitra and Govind (1981, 1985) considered a series of recycle reactors, and they optimized the recycle ratio and the point of recycle. Balakrishna and Biegler (1993) described a superstructure for the simultaneous synthesis of reaction, energy, and separation systems. Kokossis and Floudas (1990, 1994) considered a large superstructure of isothermal and nonisothermal PFRs and CSTRs, formulated as a mixed integer nonlinear programming (MINLP) problem. Marcoulaki and Kokossis (1999) describe the application of stochastic optimization to find performance targets for chemical reactors followed by formulation of reactor configurations to achieve these targets.

A method that has gained prominence in the past decade seeks *attainable regions* (ARs). This approach does not assume a reactor network *a priori*, but only the set of fundamental processes (such as reaction, mixing, and so on) that can occur. The concept was first proposed by Horn (1964) and later developed by Glasser, Hildebrandt, Feinberg and co-workers (Feinberg and Hildebrandt, 1995; Glasser et al., 1987, 1992; Hildebrandt and Glasser, 1990). Horn (1964) defines the attainable region as the collection of the objective variables, such as recycle flow rate and composition of the product, that corresponds to the totality of physically possible reactors. Glasser et al. (1987) define the attainable region as a domain in the concentration space that can be achieved by using any system of steady-flow chemical reactors, that is, by using the processes of *mixing* and *reaction*. This attainable region is sometimes called the "kinetically attainable region" to distinguish it from the "thermodynamically attainable re-

Correspondence concerning this article should be addressed to M. F. Malone.
Current address of M. F. Doherty: Dept. of Chemical Engineering, University of Santa Barbara, CA 93106.

gion," determined by equilibrium constraints (Shinnar and Feng, 1985). Glasser et al. (1987) established a set of necessary conditions for the kinetically attainable region. Currently, sufficient conditions for the attainable region are not known.

AR methods are not optimization methods. AR methods serve an important purpose of generating process alternatives at the conceptual design stage of flowsheet development. Conceptual design also involves the screening of process alternatives to find an optimal flowsheet. There are relatively few general methods available for generating reactor alternatives that involve simultaneous reaction and separation. The attainable regions method generates reactor networks that are inserted into a framework for conceptual design (such as optimization-based methods, or Douglas' hierarchical procedure (Douglas, 1988). Therefore, it is not necessary to have cost measures integrated in the AR methodology, as its main purpose is to determine process alternatives, and also to determine what is feasible and what is not.

AR methods should be considered complementary to optimization-based flowsheet synthesis methods, as they can provide insights for devising a superstructure in an optimization problem. Lakshmanan and Biegler (1996) used the attainable-region properties to formulate a reactor network and optimized it using a MINLP approach. Pahor et al. (2000) suggest an iterative procedure using attainable region analysis to update the superstructure in a MINLP formulation. An important drawback of AR methods is the difficulty in applying the geometric conditions for higher dimensions. Significant work has been published for systems that can be described in up to three dimensions, however, addressing higher dimensional problems is still a challenge. Many industrially relevant reaction systems can, nevertheless, be captured in two or three dimensional (2-D or 3-D) ARs (such as the process of manufacturing methyl acetate, MTBE, TAME, and so on, can be described by a 2-D AR). Another shortcoming of the AR methodology is that it often requires recursive solutions to verify that the AR cannot be extended. In spite of these shortcomings, the AR methodology is capable of delivering process alternatives that might otherwise be missed.

Feinberg and Hildebrandt (1997) derived properties for the boundary of the attainable region. They showed that the boundary of the attainable region is always accessible by means of elementary reactors (PFR, CSTR, and so on) taken in simple combination. Glasser et al. (1987) considered combinations of plug flow, CSTR, and recycle reactors in constructing the attainable region. This analysis was also applied to systems with 3-D attainable regions (Hildebrandt and Glasser, 1990; Godorr et al., 1994), to adiabatic systems (Hildebrandt et al., 1990; Glasser et al., 1992), and to more complex reactor systems (Glasser et al., 1994). Feinberg (2000a) showed that a differential sidestream reactor (DSR) can reside on the boundary of the attainable region only if it satisfies specific design equations that govern the precise way of adding sidestreams along the length of the reactor, and these equations depend on the reaction chemistry and kinetics. The CSTRs that give rise to extreme points of the attainable region must also conform to certain special design equations (Feinberg, 2000b). These design equations indicate that for a CSTR to give a point on the boundary of the attainable region, there are only very exceptional values of residence time (which are usually computable). Rooney et al. (2000) describe a method for constructing attainable regions of dimensions greater than two by combining 2-D projections of candidate regions. Smith and Malone (1997) applied the concept to polymerization reaction systems for determining the attainable region for number-average molecular weights and polydispersity.

The idea of combining reaction with distillation has been known for a long time (Backhaus, 1921a–d; Keyes, 1932). Nisoli et al. (1997) applied the concept of attainable region to find feasible compositions for systems with simultaneous reaction and separation in cocurrent devices. The reaction-separation devices considered were: CSTR with vapor removal and PFR with vapor removal. However, they did not estimate the conversions achieved using the reaction-separation devices. It is not known how simultaneous separation with reaction in a countercurrent device affects the region of feasible compositions. Feinberg (2001) showed that for finding bounds on the attainable effluents from reactor-separator systems of arbitrary design, it is sufficient to consider a reaction system with a finite number of CSTRs coupled with a separation system capable of making sharp separations; the number of CSTRs needed to describe the boundary of the attainable region depends on the number of independent reactions in the reaction chemistry.

In this work, we apply the attainable region methodology to a cascade of vapor-liquid CSTRs in which the liquid and vapor move in countercurrent flow. For this, as for any system with chemical reaction, the yield, selectivity, and conversion are critically important in process engineering. When a reactor system has more than one product stream, these quantities are determined from the overall compositions given by the (hypothetical) mixing of all the product streams. Since a countercurrent cascade of vapor-liquid CSTRs has both liquid and vapor products, we use these overall compositions in what follows. *The attainable region for reaction-separation should encompass all possible overall compositions achievable by using the phenomena of reaction, separation and mixing (including those obtained from hybrid devices for reaction-separation)*. We focus here only on the countercurrent cascade of two-phase CSTRs along with the single-phase CSTR and PFR. Therefore, the feasible region that we identify will be a subset of the attainable region for reaction-separation. The feasible region gives an estimate of the overall product compositions achievable using a countercurrent reaction-separation device and, therefore, provides an estimate of its potential advantage over conventional reactors.

Motivation

Consider a system with the elementary irreversible reactions in series $A \xrightarrow{k_{f,1}} B \xrightarrow{k_{f,2}} C$ in an ideal liquid solution. For simplicity, we assume that the rate constants are independent of temperature. For this reaction system, a PFR will always give better yield and selectivity to the desired product B than a CSTR (Levenspiel, 1972). When the rate constant for both the reactions are identical, the attainable region boundary is the PFR trajectory, which is convex. The CSTR locus lies inside the PFR trajectory.

Now, consider a two-phase CSTR, consisting of a flash separator with a simultaneous chemical reaction in the liquid

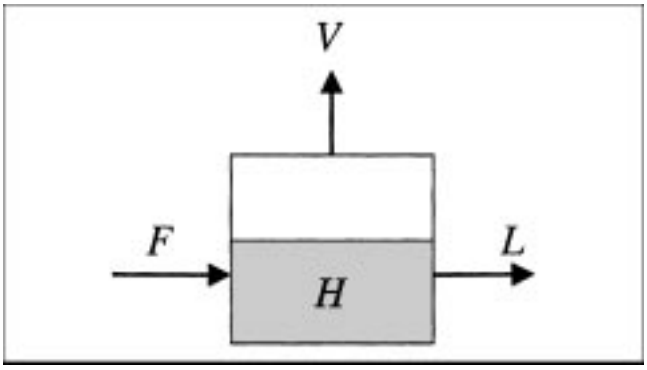

Figure 1. CSTR with vapor removal.

phase, as shown in Figure 1. We assume that the liquid and vapor are in phase equilibrium, and that the volatilities of components B and C relative to A are constant and equal to 5 and 3, respectively. Therefore, the vapor in phase equilibrium with the liquid reaction mixture will have more of the desired product B compared to the liquid phase. It is intuitive that removing vapor from a CSTR will help in removing the desired product from the reaction mixture and is bound to improve the selectivity for the process. A model is developed for the device in Figure 1 to calculate the yield of B and selectivity to B with the conversion of A. Activity-based rate expressions are used in formulating the model for reasons explained in Nisoli et al. (1997).

The overall material balance (Figure 1) is written as

$$F - L - V + \sum_{k=1}^{2} \nu_{T,k} r_k(x) H = 0 \tag{1}$$

where $r_k(x)$ is the reaction rate per mol of liquid mixture for the kth reaction, and has the dimensions of mols reacted per mol of mixture per unit time. $\nu_{T,1}$ and $\nu_{T,2}$ are the algebraic sum of the stoichiometric coefficients for the first and second reaction, respectively. The streams F and L are assumed to be saturated liquids. The material balance for the ith component is

$$Fx_{i,0} - Lx_i - Vy_i + \sum_{k=1}^{2} \nu_{i,k} r_k(x) H = 0 \tag{2}$$

The vapor compositions are determined by using a constant relative volatility model. Since both reactions are equimolar $\nu_{T,1} = \nu_{T,2} = 0$. Eliminating L from Eqs. 1 and 2, we obtain

$$x_i - x_{i,0} = \frac{V}{F}(x_i - y_i) + \frac{H}{F} \sum_{k=1}^{2} \nu_{i,k} r_k(x) \tag{3}$$

The Damköhler number (Damköhler, 1939) $Da = Hk_{f,\mathrm{ref}}/F$ is the ratio of a characteristic liquid residence time (H/F) to the characteristic reaction time ($1/k_{f,\mathrm{ref}}$), where $k_{f,\mathrm{ref}}$ is the rate constant for the reference reaction. $\Phi = V/F$ is the fraction of liquid feed that is vaporized. Using these parameters

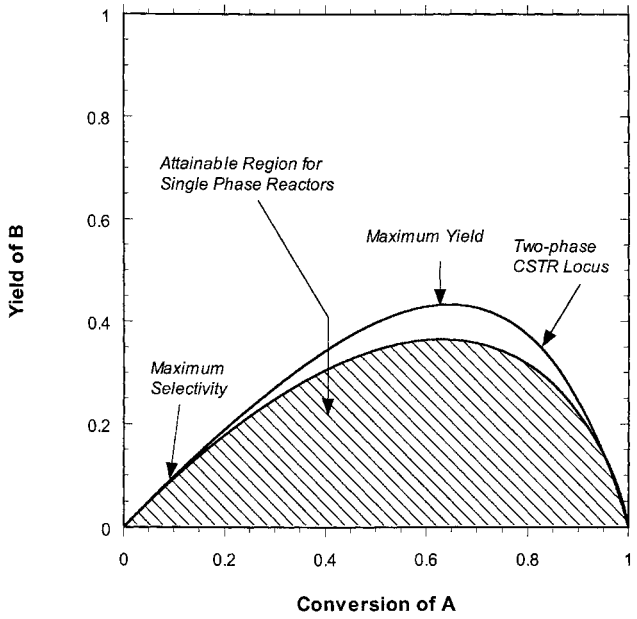

Figure 2. Separation effect on attainable region for single-phase reactors (hatched region) for $A \rightarrow B \rightarrow C$.

in Eq. 3, we obtain

$$x_i - x_{i,0} = \Phi(x_i - y_i) + Da \sum_{k=1}^{2} \nu_{i,k} \frac{r_k(x)}{k_{f,\mathrm{ref}}} \tag{4}$$

The difference between the liquid composition vectors $\boldsymbol{x}$ and $\boldsymbol{x}_0$ is given in terms of a separation vector $(\boldsymbol{x} - \boldsymbol{y})$ and a reactor vector $\Sigma_{k=1}^{2} \boldsymbol{\nu}_k r_k(\boldsymbol{x})$. Given a value for F, a choice of Φ sets all of the flows and Da determines the reactor volume. The yield of the desired product B and the conversion of A is found from the combined streams L and V, and the overall outlet composition vector is given by $(1-\Phi)\boldsymbol{x} + \Phi \boldsymbol{y}$. The selectivity to B is simply the ratio of yield of B to conversion of A.

We use first-order reaction rate models for both reactions, where the rates are given as: $r_1(x) = k_{f,1} x_A$ and $r_2 = k_{f,1} x_A - k_{f,2} x_B$. We choose $\Phi = 0.8$, and a liquid feed of pure A to the two-phase CSTR. Assuming that the rate constant for both reactions is identical, $k_{f,1} = k_{f,2} = k_{f,\mathrm{ref}}$, the conversion of A, the yield and selectivity to B are determined from the overall composition vector after specifying a value for Da and solving Eq. 4. The conversion increases monotonically with Da since the characteristic residence time increases for a given characteristic reaction time. Figure 2 shows the yield of B vs. the conversion of A for the two-phase CSTR. The hatched area is the attainable region for single-phase reactors (CSTR, PFR). The figure shows that using a CSTR with vapor removal gives a larger region of feasible overall compositions than for single-phase reactors. Figure 3 shows the selectivity to B vs. the conversion of A. Good improvement in selectivity is possible by using a two-phase CSTR over a conventional reactor. Since the desired product, B is the lightest boiling component in the mixture, vaporization improves yield

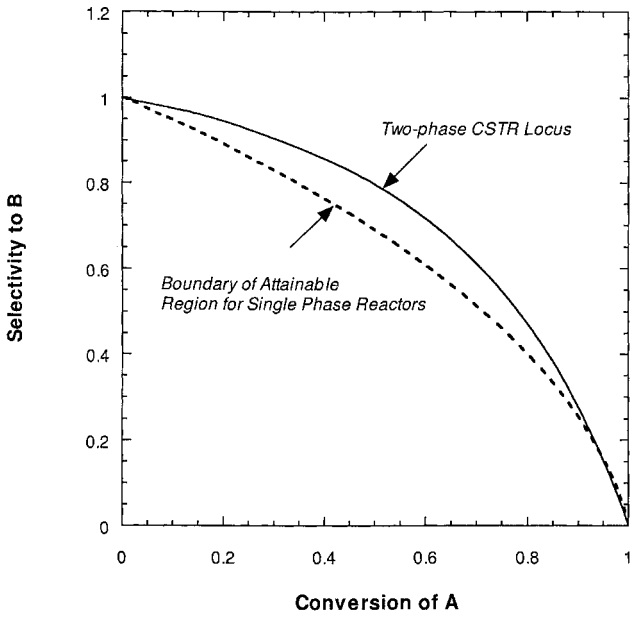

Figure 3. Selectivity to *B* vs. conversion of *A* for two-phase CSTR and boundary of attainable region for single-phase reactors.

and selectivity to B. It is therefore logical to string together a series of CSTRs where the liquid and vapor streams move in a countercurrent fashion. Such a configuration can also be expected to increase the conversion in equilibrium limited reactions.

Model Development for Countercurrent Cascade of Two-Phase CSTRs

Figure 4 shows a countercurrent cascade of two-phase CSTRs, which is a surrogate for the rectifying or stripping sections of a reactive distillation column. We develop a model for c components and R reactions in a cascade of N vapor-liquid CSTRs. The reactions are assumed to occur only in the liquid phase and the cascade is isobaric. The overall material balance on stage j (Figure 4) is

$$L_{j-1} - L_j + V_{j+1} - V_j + \sum_{k=1}^{R} \nu_{T,k} r_k(\boldsymbol{x}_j) H_j = 0 \qquad (5)$$

where $r_k(\boldsymbol{x}_j)$ is the reaction rate of reaction k per mol of liquid mixture in stage j and has the dimensions of mols reacted per mol of mixture per unit time, and $\nu_{T,k}$ is the algebraic sum of the stoichiometric coefficients in reaction k. The material balance for component i on stage j is

$$L_{j-1}x_{i,j-1} - L_j x_{i,j} + V_{j+1}y_{i,j+1} - V_j y_{i,j} + \sum_{k=1}^{R} \nu_{i,k} r_k(\boldsymbol{x}_j) H_j; \qquad i = 1, \ldots, c-1 \quad (6)$$

We assume that the liquid composition is related to the vapor composition by vapor liquid equilibrium. The temperature of the reaction mixture is determined by phase equilibrium, and the energy balance is only needed when heating or cooling policy is to be calculated, which can be done separately.

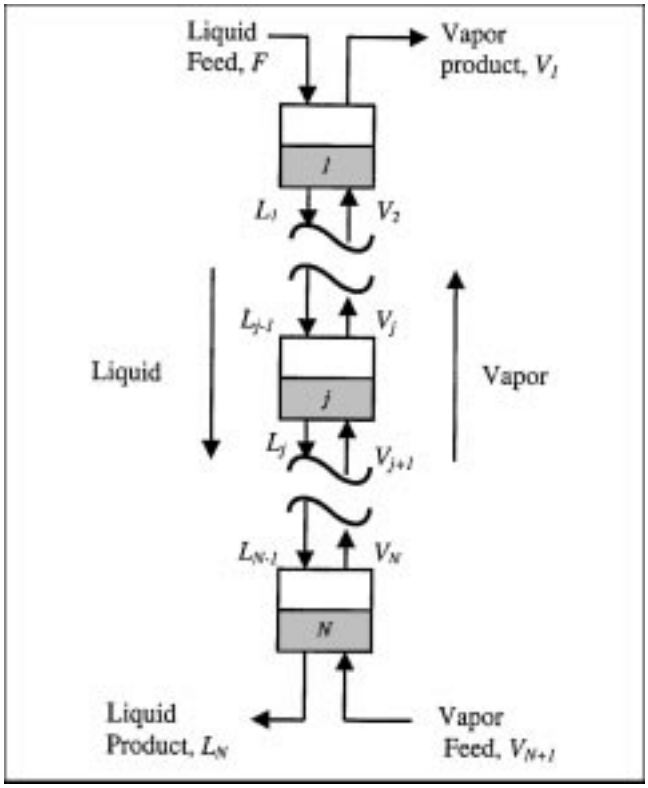

Figure 4. Countercurrent cascade of two-phase CSTRs.

Eliminating L_j from Eqs. 5 and 6, we obtain

$$x_{i,j} - x_{i,j-1} = \frac{V_j}{L_{j-1}}(x_{i,j} - y_{i,j}) - \frac{V_{j+1}}{L_{j-1}}(x_{i,j} - y_{i,j+1}) + \frac{H_j}{L_{j-1}} \sum_{k=1}^{R} (\nu_{i,k} - \nu_{T,k} x_{i,j}) r_k(\boldsymbol{x}_j); \qquad i = 1, \ldots, c-1 \quad (7)$$

The molar liquid holdup on stage j is $H_j = \rho_j \upsilon_j$, where ρ_j is the molar density of the liquid mixture and υ_j is the volume of the liquid phase on stage j. It is convenient to rewrite the molar quantities L_{j-1}, V_j, V_{j+1} and ρ_j in terms of the corresponding mass quantities L^m_{j-1}, V^m_j, V^m_{j+1} and ρ^m_j, giving

$$x_{i,j} - x_{i,j-1} = \frac{V^m_j}{L^m_{j-1}} \frac{M(\boldsymbol{x}_{j-1})}{M(\boldsymbol{y}_j)}(x_{i,j} - y_{i,j}) - \frac{V^m_{j+1}}{L^m_{j-1}} \frac{M(\boldsymbol{x}_{j-1})}{M(\boldsymbol{y}_{j+1})}(x_{i,j} - y_{i,j+1}) + \frac{\rho^m_j \upsilon_j}{L^m_{j-1}} \frac{M(\boldsymbol{x}_{j-1})}{M(\boldsymbol{x}_j)} \sum_{k=1}^{R} r_k(\boldsymbol{x}_j)(\nu_{i,k} - \nu_{T,k} x_{i,j}); \qquad i = 1, \ldots, c-1 \quad (8)$$

where M is the average molecular weight

$$M(\boldsymbol{x}_j) = \sum_{i=1}^{c} M_i x_{i,j} \tag{9}$$

Similar definitions apply to $M(\boldsymbol{x}_{j-1})$, $M(\boldsymbol{y}_j)$ and $M(\boldsymbol{y}_{j+1})$.

We define the following two dimensionless parameters

$$\phi_j^m = \frac{V_j^m}{L_{j-1}^m} \tag{10}$$

$$Da_j = \frac{k_{f,\mathrm{ref}}\,\rho_j^m\,\upsilon_j}{L_{j-1}^m} \tag{11}$$

We assume that $V^m = V_1^m = \cdots = V_{N+1}^m$, $F^m = L_1^m = \cdots = L_N^m$ and $\upsilon_1 = \upsilon_2 = \cdots = \upsilon_N$ so that $\phi_j^m = \phi^m$ and $Da_j = Da$ throughout the cascade; ϕ^m represents the feed flow rate ratio V^m/F^m. Here, $k_{f,\mathrm{ref}}$ is the forward rate constant for a reference reaction at a reference temperature. The following are the reasons for using mass variables instead of molar quantities:

- It is reasonable to assume the mass density of the liquid phase is approximately constant with respect to changes in the state of the system between inlet and outlet conditions.
- The total number of mols in the reaction mixture changes with conversion for a nonequimolar chemistry. If Da is defined in terms of molar quantities, it is not possible to assume a constant value for Da. However, Da can be assumed to be constant throughout the cascade by defining it in mass variables, as in Eq. 11.

Using the dimensionless quantities ϕ^m and Da in Eq. 8, we get

$$\begin{aligned} x_{i,j} - x_{i,j-1} = {} & \phi^m \frac{M(\boldsymbol{x}_{j-1})}{M(\boldsymbol{y}_j)}(x_{i,j} - y_{i,j}) \\ & - \phi^m \frac{M(\boldsymbol{x}_{j-1})}{M(\boldsymbol{y}_{j+1})}(x_{i,j} - y_{i,j+1}) \\ & + Da \frac{M(\boldsymbol{x}_{j-1})}{M(\boldsymbol{x}_j)} \sum_{k=1}^{R} \frac{r_k(\boldsymbol{x}_j)}{k_{f,\mathrm{ref}}}(\nu_{i,k} - \nu_{T,k} x_{i,j}); \\ & i = 1, \ldots, c-1;\ j = 1, \ldots, N \end{aligned} \tag{12}$$

The material balance Eqs. 12 are coupled nonlinear algebraic equations. For a large number of stages, the problem is large and difficult to converge using solvers like DNEQNF (IMSL subroutine based on the Newton's method) or HYBRD (modification of the Powell hybrid method). Compared to nonlinear algebraic solvers, solvers for nonlinear differential equations (for instance LSODES, Livermore solver for ordinary differential equations) are more robust for large systems of equations. We therefore convert Eq. 12 into differential equations and solve them until they reach a steady state. The advantage of this method is exemplified later in the article, where the nonlinear algebraic solver fails, but the differential equation solver yields converged results. Equation 12 can be written as

$$\begin{aligned} \frac{dx_{i,j}}{d\xi} = {} & x_{i,j-1} - x_{i,j} + \phi^m \frac{M(\boldsymbol{x}_{j-1})}{M(\boldsymbol{y}_j)}(x_{i,j} - y_{i,j}) \\ & - \phi^m \frac{M(\boldsymbol{x}_{j-1})}{M(\boldsymbol{y}_{j+1})}(x_{i,j} - y_{i,j+1}) \\ & + Da \frac{M(\boldsymbol{x}_{j-1})}{M(\boldsymbol{x}_j)} \sum_{k=1}^{R} \frac{r_k(\boldsymbol{x}_j)}{k_{f,\mathrm{ref}}}(\nu_{i,k} - \nu_{T,k} x_{i,j}); \\ & i = 1, \ldots, c-1;\ j = 1, \ldots, N \end{aligned} \tag{13}$$

For equimolar reaction chemistries, the molar holdup on each stage can be taken as constant, $H_j = H$. We simplify the model in Eq. 13 by defining the following dimensionless parameters

$$\phi_j = \frac{V_j}{L_{j-1}} \tag{14}$$

$$Da = \frac{k_{f,\mathrm{ref}} H}{L_{j-1}} \tag{15}$$

ϕ represents the feed flow rate ratio V/F. We assume that $V = V_1 = \cdots = V_{N+1}$ and $F = L_1 = \cdots = L_N$, so that the value of ϕ and the Damköhler number Da do not vary with position throughout the cascade. This corresponds to constant molar flows through the cascade, which can be achieved when the cascade is adiabatic, the heat of vaporization is constant, and the heat of reaction is negligible. A constant molar flows model is usually a good starting point for conceptual design. For the examples considered in this article, the heat of reaction is insignificant. However, for reaction systems where the heat of reaction is not negligible compared to the heat of vaporization, the model must be modified to account for the energy balance equations throughout the cascade. Chen et al. (2000) published a heat effects model for the simulation of a reactive distillation column, and a similar approach can be used to model a countercurrent cascade when heat effects are significant. Methods for incorporating differences in the heats of vaporization to improve the fidelity of the constant molar overflow models are given in Doherty and Malone (2001), and can be applied to the models developed in this article.

For equimolar reactions, the model given in Eq. 13 simplifies to the following

$$\begin{aligned} \frac{dx_{i,j}}{d\xi} = {} & x_{i,j-1} - x_{i,j} + \phi(y_{i,j+1} - y_{i,j}) + Da \sum_{k=1}^{R} \nu_{i,k} \frac{r_k(\boldsymbol{x}_j)}{k_{f,\mathrm{ref}}}; \\ & i = 1, \ldots, c-1;\ j = 1, \ldots, N \end{aligned} \tag{16}$$

We use this model throughout the article. If there is a single stage in the cascade and $\phi = 0$, the configuration is equivalent to a single-phase CSTR. In the case where there are large number of stages in the cascade and $\phi = 0$, the configuration is equivalent to a single-phase plug-flow reactor. A countercurrent cascade is a multifunctional reactor that can potentially give higher conversions in equilibrium limited reactions, and better selectivities for systems with side reac-

tions. It cannot, however, give pure products at both ends since the feeds are at the top and bottom ends. Therefore, in a flowsheet, a countercurrent cascade has to be matched with a conventional separation system to get pure products. The flowsheet alternatives involving countercurrent cascades should be compared with the conventional reactor followed by separation flowsheets to identify an optimal flowsheet.

Overall Composition Vector

The system shown in Figure 4 has a liquid and a vapor feed. The products exit stage 1 as vapor and stage N as liquid. These product compositions depend on the composition of the feedstreams, on the parameters Da and ϕ, and also on the number of stages N. For quantifying the performance of the device, we use the indicators conversion, yield, and selectivity. These indicators are calculated from the overall product compositions achieved by a simultaneous reaction-separation system. In this case, the overall composition is determined by mixing the liquid product with condensed vapor product. The overall feed composition vector $\bar{\boldsymbol{x}}_0$, for the system shown in Figure 4 is

$$\bar{\boldsymbol{x}}_0 = \frac{1}{1+\phi}\boldsymbol{x}_0 + \frac{\phi}{1+\phi}\boldsymbol{y}_{N+1} \tag{17}$$

From Eq. 16, the overall product composition vector for the cascade is

$$\bar{\boldsymbol{x}} = \frac{1}{1+\phi}\boldsymbol{x}_N + \frac{\phi}{1+\phi}\boldsymbol{y}_1 \tag{18}$$

Note that ϕ can take values from 0 to ∞, while, for the device shown in Figure 1, we use Φ to denote the ratio of vapor rate to feed rate, which takes values from 0 to 1. We normalize the value of ϕ by defining

$$\Phi = \frac{\phi}{1+\phi} \tag{19}$$

Equations 17 and 18 can be rewritten as

$$\bar{\boldsymbol{x}}_0 = (1-\Phi)\boldsymbol{x}_0 + \Phi\boldsymbol{y}_{N+1} \tag{20}$$

$$\bar{\boldsymbol{x}} = (1-\Phi)\boldsymbol{x}_N + \Phi\boldsymbol{y}_1 \tag{21}$$

The overall composition vectors given by Eqs. 20 and 21 are used for calculating conversion, yield, and so on, for the countercurrent cascade of two-phase CSTRs. The difference vector for overall composition is given as

$$\bar{\boldsymbol{x}} - \bar{\boldsymbol{x}}_0 = \boldsymbol{f}(Da, \boldsymbol{x}_0, \boldsymbol{y}_{N+1}, \phi, N) \tag{22}$$

The function $\boldsymbol{f}$ is the combined effect of reaction and separation in the N stages of the system in Figure 4. Since both the overall feed composition and overall product composition are attainable, all compositions on the difference vector are attainable. For a single-phase CSTR, the difference vector for compositions is written as

$$\boldsymbol{x} - \boldsymbol{x}_0 = \boldsymbol{r}(\boldsymbol{x})\tau \tag{23}$$

Therefore,

$$\boldsymbol{x} - \boldsymbol{x}_0 = \boldsymbol{g}(\tau, \boldsymbol{x}_0) \tag{24}$$

where τ is the residence time for the CSTR, and $\boldsymbol{g}$ is the reaction vector for a CSTR. The righthand side of Eqs. 22 and 24 are a set of nonlinear algebraic equations, therefore, they have the same mathematical structure. Therefore, the difference vector for overall composition in a cascade of two phase CSTRs is collinear with the reaction-separation vector (which is given by $\boldsymbol{f}$). A locus for Eq. 22 is found by determining the overall composition difference vector at all values of Da.

We use the following necessary conditions of the attainable region for single-phase reactors (Glasser et al., 1987) in finding the feasible region for the cascade of vapor-liquid CSTRs:

- The region is convex, that is, a line that joins any two compositions in the region also lies inside the region;
- No reaction-separation vector on the boundary of the region points outward from the region, that is, the reaction-separation vector at the boundary either points inward, is tangent, or has a zero magnitude.

The lack of sufficient conditions does not have any impact on the acceptability of the candidate attainable region (in our case, the feasible region). It only means the region and the reactor networks identified are open to further improvement. The overall feed and product compositions for the cascade are used to determine conversion of the limiting reactant, yield (ratio of the mols of desired product formed to the mols of the limiting reactant in the overall inlet), and selectivity (ratio of the mols of desired product formed to the mols of the limiting reactant consumed).

Example 1: Reactions in Series

For the system of consecutive reactions, $A\ (1) \overset{k_f}{\rightarrow} B\ (2) \overset{k_f}{\rightarrow} C\ (3)$, the material balance equations for each stage in the cascade are given by Eq. 16. The rate constant for both the reactions is equal, however, this analysis can be repeated for cases where rate constants are not equal. Using the same rate and VLE models described earlier, the maximum yield of B using single-phase reactors is 0.368 shown by the attainable region for single-phase reactors in Figure 2; a PFR trajectory gives the boundary of the region. For a series reaction system with temperature independent rate constants, a mathematical proof showing that a PFR trajectory lies on the boundary of the attainable region for single-phase reactors can be found in Gadewar (2001).

To construct the feasible region for the countercurrent cascade we should consider all combinations of ϕ (ratio of vapor to liquid feed rate) and N (number of stages in the cascade). For demonstration of the concept, $\phi \leq 5$ is chosen, and the vapor feed and liquid feed to the cascade are chosen to be pure A. These constraints are relaxed later in the article. The dimension of the feasible region is 2 (see Appendix for discussion), the axes are chosen to be the conversion of A and the yield of B. The value of $\phi = 0$ for a single-stage corresponds to a CSTR which lies in the interior of the attain-

able region for single-phase reactors, while $\phi = 0$ for a large number of stages in the cascade corresponds to a PFR, which lies on the boundary of the attainable region for single-phase reactors. The PFR trajectory is convex, and is shown in Figure 5. For any given N, the locus for the countercurrent cascade of two-phase CSTRs at any $\phi < 5$ lies inside the locus for $\phi = 5$. Therefore, the value of ϕ is fixed at 5 for the subsequent analysis.

The cascade material balances given by Eq. 16 are solved for different values of Da. Each value of Da corresponds to a specific residence time and, hence, a specific conversion. The locus for a cascade with 50 stages is shown in Figure 5, no change is observed in the locus by using more stages. The overall composition achieved by mixing the liquid and vapor product is used to determine yield and conversion. The locus for a two-stage cascade extends the region the most after the yield drops down for the cascade with 50 stages. A mixing line between the trajectories for vapor-liquid cascades with 2 stages and 50 stages is given by the line *a-b*. Each point on the boundary is checked for extending the boundary using a single-phase PFR or a CSTR. A PFR starting at point *c* on the locus for the two-stage cascade extends the boundary of the feasible region. Under the constraints $\phi \leq 5$, and pure A feeds, the feasible region is given by the region *o-a-b-c-d-o* in Figure 5a. The boundary of the feasible region under constraints given in Figure 5a is formed by a locus *o-a* for a cascade with 50 stages, mixing line *a-b* between point *a* on the locus for a cascade with 50 stages and point *b* for a cascade with 2 stages, locus *b-c* for the cascade with two stages, a single-phase PFR trajectory *c-d* starting from point *c* on the locus for a cascade with two stages. There is a significant improvement in the yield of B over a single-phase PFR. Also, since selectivity is the ratio of yield to conversion, higher selectivities are obtained by using the reactor network in Figure 5b that gives the boundary of the region shown in Figure 5a.

We now relax one of the constraints regarding the feed composition to the cascade. Each point inside the feasible region *o-a-b-c-d-o* in Figure 5a can be used as a liquid and/or vapor feed to a cascade of two-phase CSTRs. The mol fractions corresponding to point *e* on the boundary of the region in Figure 6 is chosen to be the feed composition for vapor and liquid in a cascade with 50 stages. *Curve 1* corresponds to this cascade and expands the feasible region under the constraint $\phi \leq 5$. Similarly, *Curve 2* for a cascade starting at point *f* also extends the boundary of the feasible region given in Figure 5a. We can carry out this exercise by using a cascade with other feed compositions lying on the boundary to form a new region and follow the same procedure for the boundary of the new region.

Figure 5a shows that at low conversions, the locus for a cascade with a large number of stages is equivalent to the locus for a two-stage cascade. Also, at low conversions, the locus for a single stage is equivalent to the locus for a large number of stages. A system consisting of countercurrent cascades of two-phase CSTRs connected in series (that is, products from a cascade of CSTRs is fed to another cascade, and so on) can be closely approximated by using an arrangement shown in Figure 7, where two-phase CSTRs are connected as a cocurrent cascade. A low value of Da is chosen for each CSTR; the conversion increases with the number of CSTRs in the cocurrent arrangement. The overall composition difference vector is calculated for the cocurrent cascade of two-phase CSTRs using Eq. 4, and this vector is tangent to the overall composition trajectory (since products from each vapor-liquid CSTR are fed to the next one in the cascade, and we plot the overall composition of mixing the liquid product with condensed vapor product). Note that the relation between Φ used in Eq. 4 and ϕ used in Eq. 16 is $\Phi = (\phi/(\phi + 1))$. For a value of $\phi = 5$, $\Phi = 0.834$. Figure 8 shows the new feasible region with the boundary given by the trajectory for the cocurrent cascade of two-phase CSTRs (Figure 7). This region is convex and cannot be extended by using either a countercurrent cascade of two-phase CSTRs or single-phase reactors from its boundary. Therefore, Figure 8 shows the largest feasible region that we are able to determine for the system under the constraint $\phi \leq 5$.

We now remove the constraint on the value of ϕ. Since the boundary of the feasible region is given by the configuration in Figure 7, we use Eq. 4 for different values of Φ. Figure 9

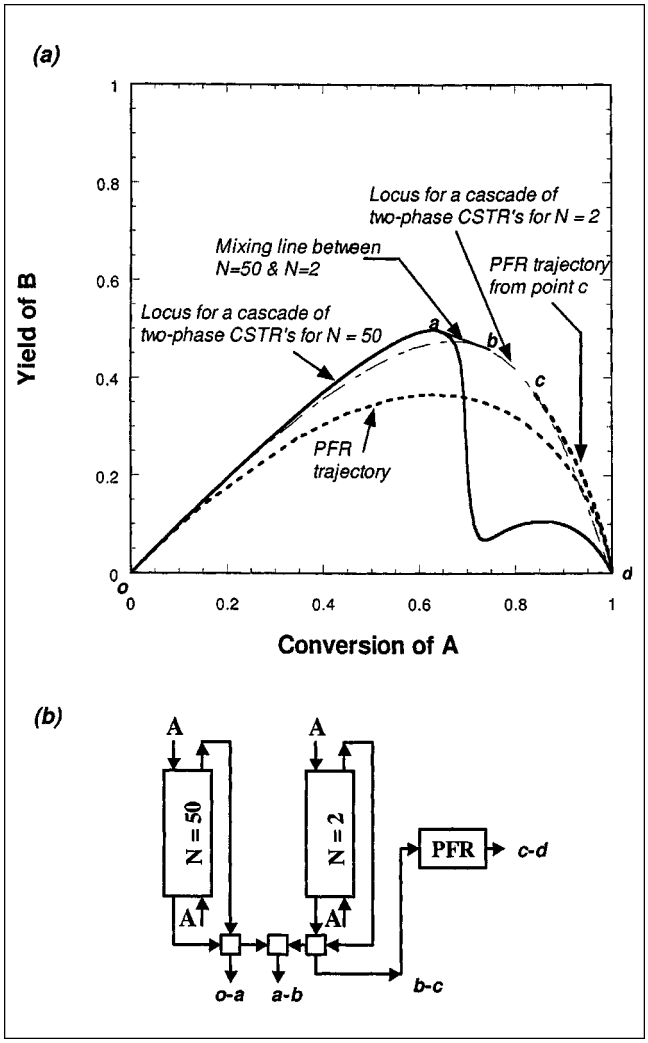

Figure 5. (a) Locus of overall yield of *B* for reactions-in-series; (b) structure on boundary of feasible region.

In (a) feasible region for the cascade under the constraints: $\phi \leq 5$, feed of pure A, is given by the region *o-a-b-c-d-o*.

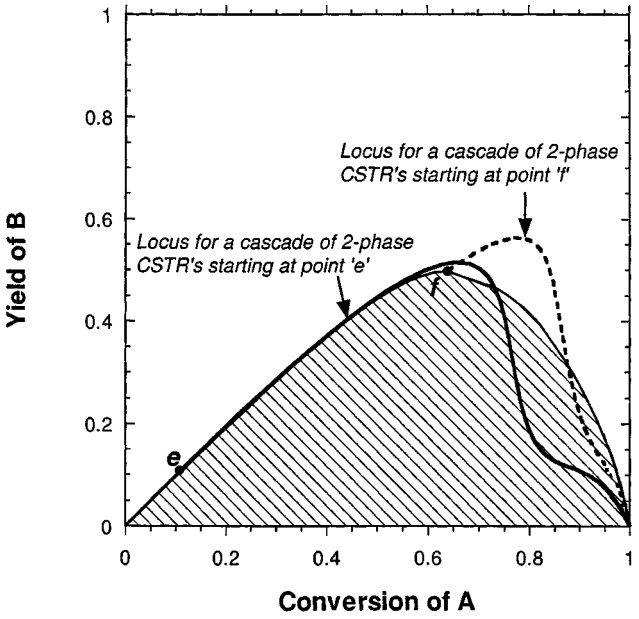

Figure 6. Locus of overall products for cascades starting on boundary of feasible region ($\phi \leq 5$).

Hatched region represents feasible region *o-a-b-c-d-o* in Figure 5a.

shows a trajectory for the cocurrent cascade of two-phase CSTRs for $\Phi = 0.999$ (equivalent to $\phi = 1{,}000$). There is no change in the trajectory for higher values of Φ. Therefore, the feasible region for a countercurrent cascade of vapor-liquid CSTRs is bounded by the trajectory for vapor-liquid CSTRs in series, shown in Figure 9. A comparison of the selectivity of B corresponding to the boundary of the feasible region and that for a single-phase PFR is shown in Figure 10. The selectivity to B is high even at higher conversions by using a countercurrent cascade of CSTRs. This analysis can provide an estimate of the raw material savings by using simultaneous reaction-separation in a countercurrent device, and, therefore, the economic incentive for implementing such a configuration. For a 95% selectivity, the single-phase reactor network can be operated at a maximum conversion $\approx 10\%$, however, to achieve the same selectivity, the reactor network consisting of countercurrent cascades can be operated at a maximum conversion $\approx 40\%$. Higher conversions significantly reduce the recycle flows and also the flow rates entering the separation system of a process. Therefore, significant savings in the separation system costs can be expected by using countercurrent cascades of two-phase CSTRs to carry out the reactions. The relative volatilities in this example are favorable for reactive separation, since the desired product gets removed during vaporization. In a case where the relative volatilities were such that the desired product B is a heavy component, and the undesired product C is the lightest component, the reactive-separation alternatives will not extend the AR for single-phase reactors. Therefore, there is no incentive in considering process alternatives consisting of countercurrent cascades of vapor-liquid CSTRs over conventional reactors (Gadewar, 2002). Therefore, the AR methodology is not only useful at the conceptual design stage to give potentially promising process alternatives, but also determines when simultaneous reaction and separation is not a good idea.

For simplicity, the rate constants in this example are assumed to be temperature independent. The reaction temperature in any stage of the countercurrent cascade is the boiling point of the mixture in that stage. The methodology outlined does not need the assumption of temperature-independent rates and can be used in cases with temperature-dependent rate constants (see Example 3). The calculation of the attainable region for single-phase reactors will, however, require the consideration of the temperature range over which the reactions are carried out. The boundary of the attainable region for single-phase reactors, therefore, might be different from the trajectory for an isothermal PFR in such cases (Glasser et al., 1992).

Yields and selectivities even higher than those obtained by reactive-separation systems are achievable using hybrid reaction-separation devices, where a nonreactive separation system removes the desired product as it is formed (Gadewar et al., 2000). Therefore, the feasible region in Figure 9 can be extended by using other hybrid reaction-separation devices. Attainable region analysis for reaction-separation should entail consideration of all reactive separation devices physically possible.

Example 2: Transalkylation of Toluene

The process of transalkylation or disproportionation of toluene is used to produce benzene and xylenes (Holmgren et al., 1999). The reaction is given as

$$2\ \text{toluene}\ (2) \rightleftharpoons \text{benzene}\ (1) + \text{xylene}\ (3) \qquad (25)$$

where (1) benzene is the lightest, (2) toluene is intermediate, and (3) xylene is the heaviest boiling. The liquid mixture is

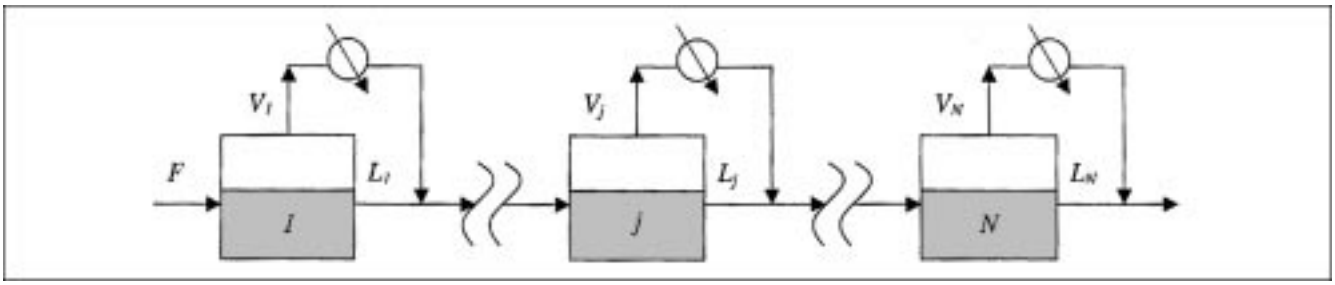

Figure 7. Cocurrent cascade of two-phase CSTRs.

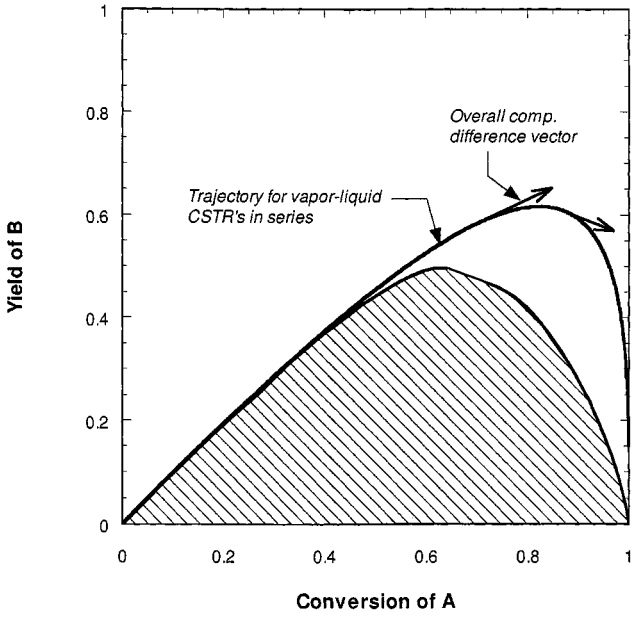

Figure 8. Feasible region for $\phi \leq 5$ with boundary of the region given by two-phase CSTRs in series.

Hatched region represents feasible region *o-a-b-c-d-o* in Figure 5a.

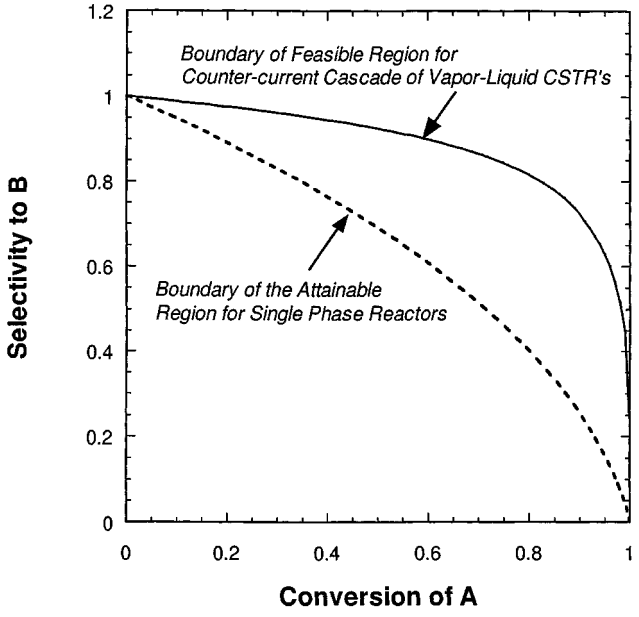

Figure 10. Improvement of selectivity to *B* using countercurrent cascades over conventional reactors.

assumed to be ideal and a constant relative volatility model is used for the VLE calculations (the *y-x* behavior determined using the NRTL equation for liquid-phase activity coefficients matches the constant relative volatility model at low pressures). The volatilities of benzene, and toluene relative to xylene are 4.8 and 2.3, respectively. The value of the equilibrium constant is taken to be $K_{\text{eq}} = 0.1$ (Buzad and Doherty, 1995). Since the reaction is equimolar, we use the model

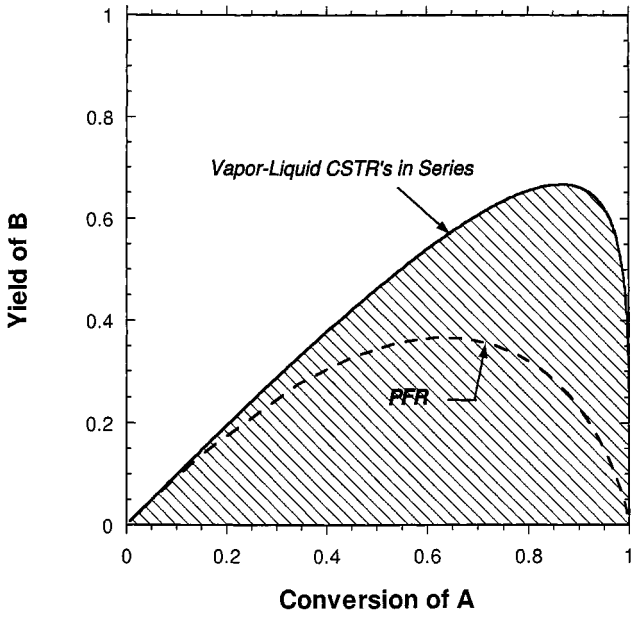

Figure 9. Feasible region (hatched region) for reactions-in-series without constraints.

given in Eq. 16, and the dimensionless parameters defined in Eqs. 14 and 15. The expression for the reaction rate is

$$r(\boldsymbol{x}_j) = k_f \left(x_{2,j}^2 - \frac{1}{K_{\text{eq}}} x_{1,j} x_{3,j} \right), j = 1, \ldots, N \qquad (26)$$

We take k_f to be independent of temperature, therefore, $k_{f,\text{ref}} = k_f$. The products from a single-phase reactor for a very large residence time lie on the equilibrium curve shown in Figure 11. Any combination of the single-phase reactors will not allow the trajectory to cross the equilibrium curve. For a feed consisting of pure toluene, the dimension of the feasible region is 1 and the region lies on the stoichiometric line with a slope $= -1/2$. For the countercurrent cascade, a similar rule applies since we plot the overall compositions after mixing the liquid product with the condensed vapor product. If the feed consists of pure toluene, the attainable region for single-phase reactors is given by the line *a-b*, where point *b* can be reached using a CSTR or a PFR with a large Damköhler number (residence time). Using a countercurrent cascade of vapor-liquid CSTRs allows conversions beyond the equilibrium curve due to simultaneous reaction and separation. Using pure toluene as the vapor and liquid feed to the cascade, the attainable region can be extended along the stoichiometric line. The feasible region is given by line *a-c* in Figure 11. The point *c* is achieved at a large value of *Da*, large number of stages (> 40) and a value of $\phi = 1$ ($L = V$). At any other values of ϕ, the region cannot be extended beyond *c*. Also, using another cascade at point *c* does not extend the feasible region.

To make the example more interesting, we assume a feedstream of pure xylene is available, which can either be mixed with toluene as feed to the cascade or can be fed pure to the

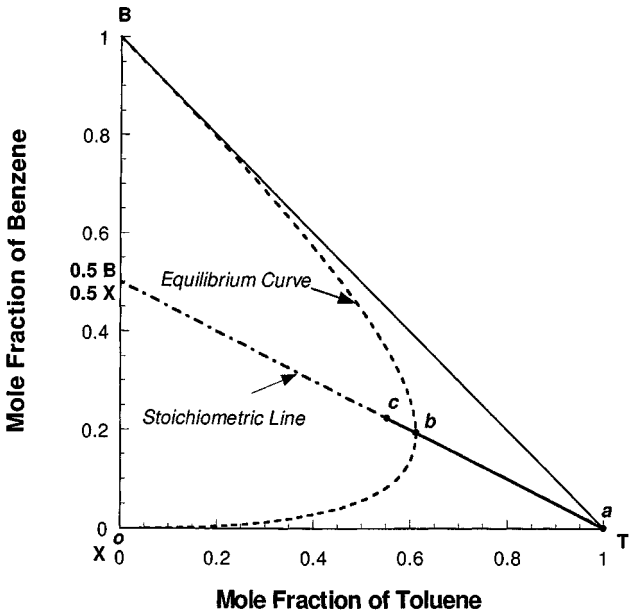

Figure 11. Locus of overall product compositions for cascade of vapor-liquid CSTRs with feed of pure toluene in transalkylation of toluene to benzene.

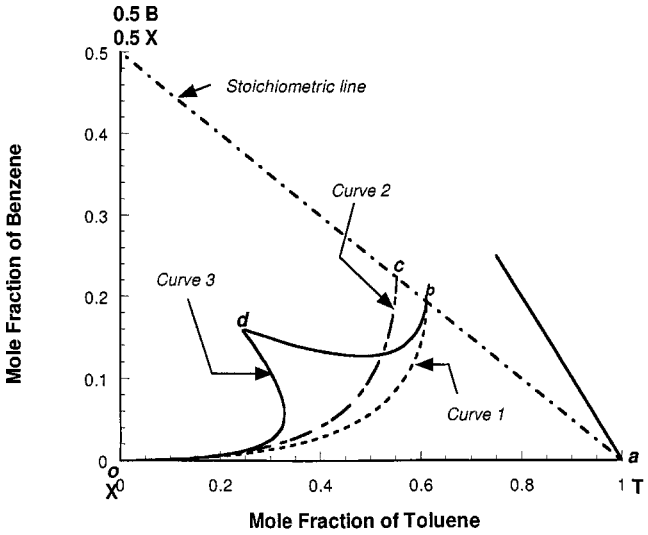

Figure 12. Locus of overall product compositions for feed consisting of toluene and xylene.

Curve 1 is the locus for single-phase reactors, *Curve 2* is the locus for cascades with mixed feeds, and *Curve 3* is the locus for cascades with pure feeds.

cascade (we will not consider a case where a pure benzene stream is also available, since the task of finding the feasible region becomes trivial; when all three components are available as pure streams, the feasible region spans the complete composition space because of mixing). This mixed feed will make the feasible region 2-D (see Appendix for details). Based on the reaction stoichiometry, the stoichiometrically feasible space is the entire triangle shown in Figure 12. The maximum value of benzene mol fraction from any reactor or reactor-separator is 0.5, which will be achieved when a feed of pure toluene is completely converted.

A single-phase reactor with a very large residence time will give products lying on the equilibrium curve, shown by *Curve 1*, in Figure 12. Consider the case when same feed composition for the vapor and liquid streams are used by choosing different feeds lying on the xylene-toluene edge. Solving Eq. 16 for each of these feeds at a large value of *Da* and at $\phi = 1$, gives *Curve 2* of the overall product compositions. At values of ϕ higher and lower than $\phi = 1$, the region cannot be expanded.

Next, we check if using pure feedstreams extends the region enclosed by *Curve 2*. Using pure toluene as the liquid feed and pure xylene as the vapor feed, the region can be extended. As the value of ϕ changes, the overall feed composition changes. At $\phi = 0$, the overall feed composition is at pure toluene and at $\phi = \infty$, the overall feed composition is at pure xylene. Solving Eq. 16 at a large value of *Da* at different values of ϕ, gives *Curve 3* of the overall product compositions. The locus for liquid feed as pure xylene and vapor feed as pure toluene, lies inside *Curve 3*. Drawing mixing lines to cover the nonconvexities in *Curve 3*, we identify a region *o-a-c-d-o* as a feasible region of overall product compositions. Using the compositions on the boundary as feed to either single-phase reactors or countercurrent cascade does not extend the feasible region. Figure 13a shows the feasible region for the system using toluene and xylene as the feed components. Point *b* corresponds to a toluene conversion of 38% and can be reached by using a single-phase reactor. Point *c* is obtained from a countercurrent cascade with pure toluene as the liquid and vapor feed, the corresponding toluene conversion is 45%. Point *d* lies on the locus for a countercurrent cascade of two-phase CSTRs with toluene as the liquid feed and xylene as the vapor feed. The corresponding toluene conversion is 56%. A flowsheet structure to access other points on the boundary of the feasible region is shown in Figure 13b.

Example 3: Synthesis of Isopropyl Acetate

Isopropyl acetate can be obtained by esterification of acetic acid with isopropanol. The reaction is

$$\text{acetic acid (HOAc)} + \text{isopropanol (IPOH)} \rightleftharpoons \text{isopropyl acetate (IPOAc)} + \text{water } (H_2O) \quad (27)$$

The thermodynamic equilibrium constant has a value of $K_{eq} = 8.7$ in the boiling temperature range of interest (Lee and Kuo, 1996; Venimadhavan et al., 1999). The kinetic model was taken from Manning (1999) for experiments performed on a heterogeneous catalyst (Amberlyst 15W, Rohm and Haas Company). A heterogeneous Langmuir-Hinshelwood/Hougen-Watson kinetic model used by Manning (1999) is

$$\mathfrak{R} = \frac{Wk'_s\left(a_{HOAc}a_{IPOH} - a_{IPOAc}a_{H_2O}/K_{eq}\right)}{\left(1 + K_{HOAc}a_{HOAc} + K_{IPOH}a_{IPOH} + K_{IPOAc}a_{IPOAc} + K_{H_2O}a_{H_2O}\right)^2} \quad (28)$$

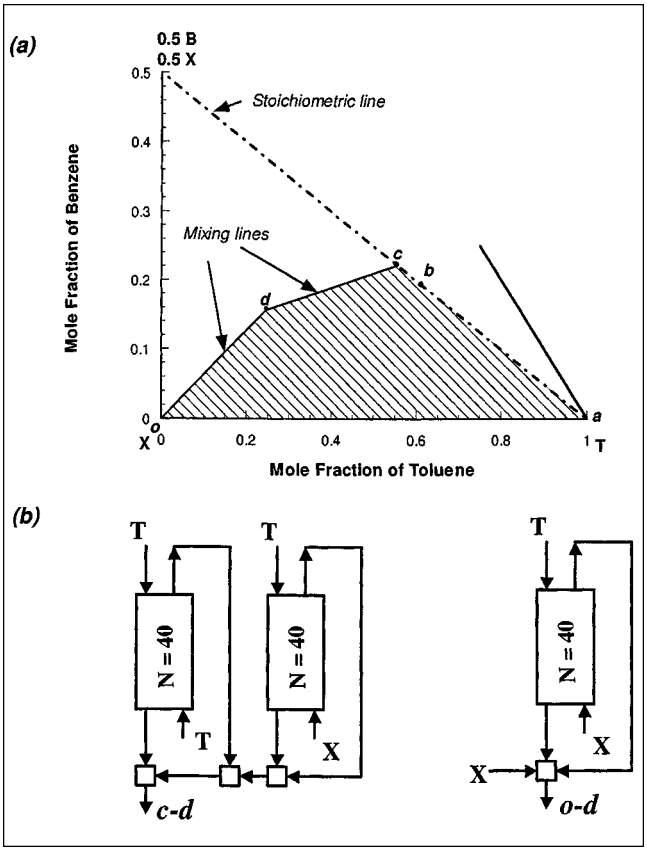

Figure 13. (a) Feasible region (hatched) for transalkylation of toluene with feed consisting of toluene and xylene; (b) structure on boundary of feasible region.

where k'_s is the apparent forward rate constant given by

$$\ln k'_s = 23.81 - \frac{8{,}253.6}{T} \tag{29}$$

Here, T is in K, and k'_s has units of mols reacted per mol of H^+ ions per minute, W is the catalyst concentration in mols of H^+ per mol of liquid mixture, and the adsorption equilibrium constants are assumed to be independent of temperature

$$K_{\mathrm{HOAc}} = 0.1976, \qquad K_{\mathrm{IPOH}} = 0.2396, \qquad K_{\mathrm{IPOAc}} = 0.147,$$

$$K_{\mathrm{H_2O}} = 0.5079 \tag{30}$$

Nonidealities are modeled using the NRTL equation (constants for Antoine equation and the NRTL binary interaction parameters are given in Table 1). The vapor-phase dimerization of acetic acid was taken into account in the VLE modeling. The Damköhler number is defined as

Table 1. Thermodynamic Data for Isopropyl Acetate Example

Component	Normal Boiling Point, °C	Antoine Coefficients a	b	c
Acetic Acid (1)	118.0	22.1001	−3,654.62	−45.392
Isopropanol (2)	82.3	22.708	−3,127.18	−75.724
Isopropyl Acetate (3)	90.3	21.487	−3,174.7	−44.601
Water (4)	100.1	23.2256	−3,835.18	−45.343

Binary Interaction Parameters for NRTL Equation

$a_{11} = 0.0$	$a_{21} = 81.3926$	$a_{31} = 154.7884$	$a_{41} = 842.6079$
$a_{12} = -281.4482$	$a_{22} = 0.0$	$a_{32} = 312.1622$	$a_{42} = 1{,}655.255$
$a_{13} = 141.0081$	$a_{23} = 379.6898$	$a_{33} = 0.0$	$a_{43} = 2{,}729.0706$
$a_{14} = -219.7238$	$a_{24} = 39.8541$	$a_{34} = 825.5563$	$a_{44} = 0.0$
$\alpha_{11} = 0.0$	$\alpha_{21} = 0.3048$	$\alpha_{31} = 0.3014$	$\alpha_{41} = 0.2997$
$\alpha_{12} = 0.3048$	$\alpha_{22} = 0.0$	$\alpha_{32} = 0.3000$	$\alpha_{42} = 0.3255$
$\alpha_{13} = 0.3014$	$\alpha_{23} = 0.3000$	$\alpha_{33} = 0.0$	$\alpha_{43} = 0.3000$
$\alpha_{14} = 0.2997$	$\alpha_{24} = 0.3255$	$\alpha_{34} = 0.3000$	$\alpha_{44} = 0.0$

Antoine Equation

$$\ln(P^{\mathrm{sat}}) = a + \frac{b}{T + c}$$

P^{sat} in Pa and T in K.

NRTL Equation

$$\ln(\gamma_i) = \frac{\sum_{j=1}^{n} \tau_{ji} x_j G_{ji}}{\sum_{k=1}^{n} x_k G_{ki}} + \sum_{j=1}^{n} \frac{x_j G_{ij}}{\sum_{k=1}^{n} x_k G_{kj}} \left(\tau_{ij} - \frac{\sum_{m=1}^{n} \tau_{mj} x_m G_{mj}}{\sum_{k=1}^{n} x_k G_{kj}} \right)$$

where

$$G_{ij} = \exp(-\tau_{ij}\alpha_{ij})$$

$$\tau_{ij} = \frac{a_{ij} + b_{ij}T}{RT} \text{ cal/gmol}$$

Note: All $b_{ij} = 0$ here.

$$Da = \frac{H/F}{1/(k'_{s,\mathrm{ref}} W)} \tag{31}$$

where $k'_{s,\mathrm{ref}}$ is the forward reaction rate constant at a reference temperature chosen as the boiling temperature of the lowest boiling component in the mixture (IPOH) at 1 atm, $T_{\mathrm{ref}} = 82.38$°C, and the corresponding $k'_{s,\mathrm{ref}} = 1.8$. The dimensionless reaction rate to be used for solving Eq. 16 is

$$\frac{r(x)}{k_{f,\mathrm{ref}}} \equiv \frac{\mathfrak{R}}{k'_{s,\mathrm{ref}} W} \tag{32}$$

We assume the reactants acetic acid and isopropanol are available as pure streams. We can use either a mixed feed to the cascade or a pure vapor and liquid feed to the countercurrent cascade. All the overall product compositions are constrained by the reaction stoichiometry to satisfy $\bar{x}_{\mathrm{IPOAc}} = \bar{x}_{\mathrm{H_2O}}$. This is a linear constraint shown by the "stoichiometric plane" in Figure 14. The dimension of the feasible region is 2,

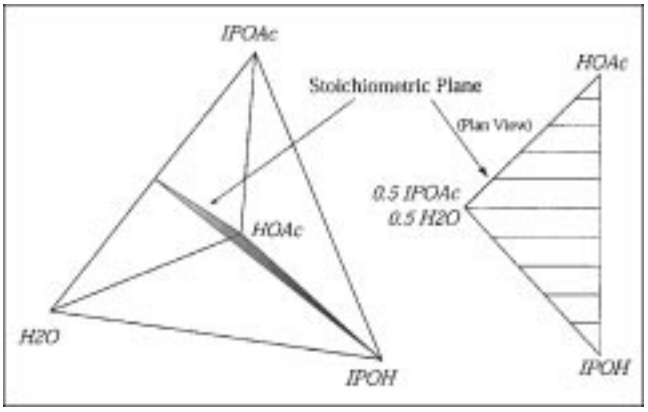

Figure 14. Stoichiometric plane inside composition space for the isopropyl acetate system.

the axes are chosen to be the mol fraction of acetic acid, and the mol fraction of isopropyl acetate. The products from a single-phase reactor for a very large residence time will lie on the equilibrium curve. The equilibrium composition depends on $K_{eq}(T)$ and on the activity coefficients, and, hence, on the temperature of the reaction mixture. When the reaction mixture is at its boiling point, the equilibrium is given by *Curve 1* in Figure 15. Based on the reaction chemistry, the overall input composition to any single-phase reactor or a cascade of two-phase CSTRs and its overall product composition lies on a line with a slope $= -1$. Also, the stoichiometrically feasible space is the entire triangle in Figure 15. The mol fraction of isopropyl acetate in the reaction mixture can be at most 0.5.

For a pure liquid feed of acetic acid and a vapor feed of pure isopropanol, *Curve 2* is the locus of the mol fraction of isopropyl acetate in the overall output from a countercurrent cascade of vapor-liquid CSTRs with a large number of stages (> 40) and a large *Da*. Each point on the *Curve 2* is at a different value of ϕ; a very low value of ϕ corresponds to the overall feed very close to the acetic acid vertex and a very large value of ϕ corresponds to an overall feed close to the isopropanol vertex shown by point *o*. Lower values of *Da* do not extend the region enclosed by *Curve 2*. A nonlinear algebraic model given by the righthand side of Eq. 16 should give the same results, however, neither of the available standard subroutiness (DNEQNF from IMSL or HYBRD from Livermore solvers) converge to solutions. One of the reasons is the failure of the VLE subroutine when the value of the liquid mol fraction exceeds unity or is a negative value, during the root-finding procedure.

Now consider the case of a mixed feed to the cascade. A mixture of acetic acid and isopropanol is used as the liquid feed and the vapor feed to the cascade. The composiiton of both feeds is the same. Equation 16 is solved for specified values of the parameters *Da*, ϕ, and *N*. The overall mol fraction of isopropyl acetate in the product increases with each of the parameters. The effect of increasing the number of stages diminishes after $N = 40$. Also, a very large value of *Da* corresponds to liquid in each stage reaching reaction equilibrium. Also, the effect of ϕ dimishes after $\phi = 100$. Therefore, we calculate the overall output mol fraction of isopropyl acetate for a cascade with a large number of stages $N > 40$,

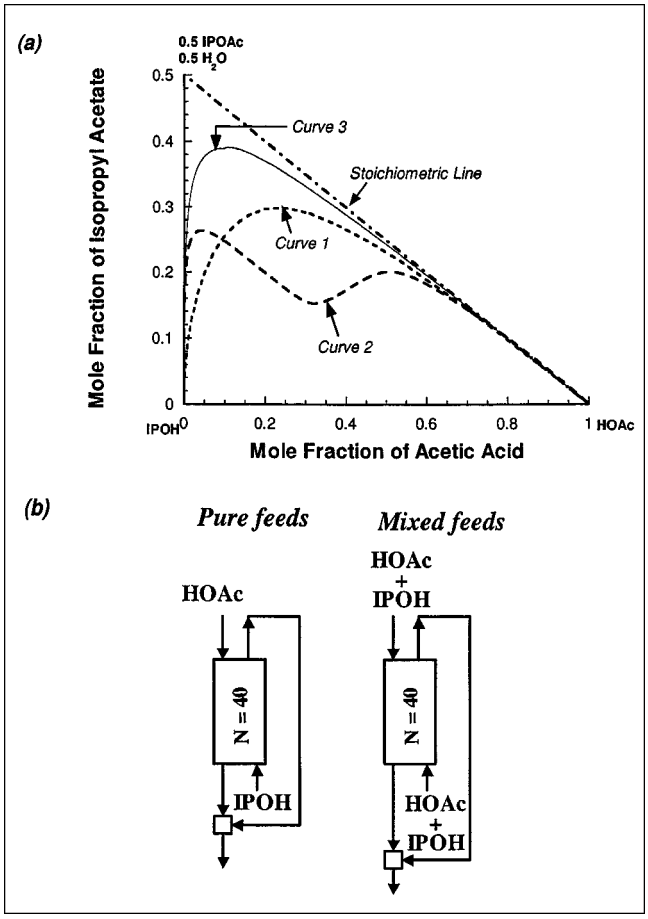

Figure 15. (a) Locus of overall product compositions for feed consisting of acetic acid and isopropanol; (b) countercurrent cascade of two-phase CSTRs for pure feeds and mixed feeds.

In (a) *Curve 1* is the locus for single-phase reactors, *Curve 2* is the locus for cascades with pure feeds, and *Curve 3* is the locus for cascades with mixed feeds.

large *Da*, and $\phi = 100$. The feed compositions are chosen along the abscissa and solve Eq. 16 at each of these feeds. The locus of the overall product mol fraction of isopropyl acetate is given by *Curve 3*. The region enclosed by *Curve 3* is convex and also encloses the locus for pure feeds, that is, *Curve 2*. The countercurrent cascade structures that give curves 2 and 3 are shown in Figure 15b. Generating each of these curves takes a couple of hours of computation time on a 450 MHz PC. In the case of an ideal VLE, the same calculations would take a few minutes. A feasible region requires some post processing once the curves are generated. When all is in, a feasible region can be generated within one day.

A single-phase reactor or reactors cannot extend the region beyond *Curve 3* since the compositions will head towards the reaction equilibrium curve. A single vapor-liquid CSTR at large vapor rates also gives overall product compositions that lie on *Curve 3*. The trajectory for a countercurrent cascade of vapor-liquid CSTRs (Figure 7) reaches *Curve 3* and then starts moving towards the equilibrium curve (along

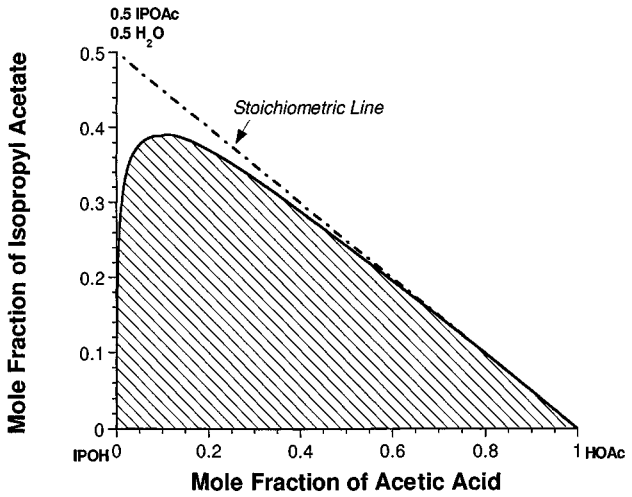

Figure 16. Feasible region for synthesis of isopropyl acetate from acetic acid and isopropanol (hatched region).

the stoichiometric line of slope -1) as the backward reaction exceeds the forward reaction. Using a cascade of two-phase CSTRs starting at any point on *Curve 3* cannot extend the region. Therefore, the region enclosed by *Curve 3* is the largest feasible region that we are able to find for this reaction system and is given in Figure 16. The boundary of the feasible region can be reached either by using a single vapor-liquid CSTR, or a countercurrent cascade of vapor-liquid CSTRs, or cocurrent cascade of vapor-liquid CSTRs (Figure 7).

Conclusions

A model for a cascade of vapor-liquid CSTRs, where the vapor and the liquid flow countercurrently, has been developed. The model is formulated using two independent dimnesionless parameters: the Damköhler number, which relates the residence time to the characteristic reaction time, and the vapor fraction ϕ, which depends on the heating policy.

We have introduced an overall composition difference vector of Eq. 22, which depends on the overall reaction and separation in the cascade. This vector obeys the same properties as the reaction vector (Glasser et al., 1987) or the reaction-separation vector (Nisoli et al., 1997). The necessary conditions for the attainable region with reaction and mixing can therefore be applied to the system with simultaneous reaction and separation.

The feasible region for a hypothetical example of reactions in series $A \rightarrow B \rightarrow C$ is bounded by the trajectory for a device consisting of cocurrent cascade of vapor-liquid CSTRs. For isopropyl acetate synthesis, the boundary of the feasible region is reached by a vapor-liquid CSTR, or by a countercurrent cascade of vapor-liquid CSTRs, or by a cocurrent cascade of vapor-liquid CSTRs at a large vapor rate. In the transalkylation of toluene, however, the feasible region boundary is given by mixing lines between products from countercurrent cascades of vapor-liquid CSTRs. The choice of a particular configuration will depend on a cost analysis. For the examples considered, we have demonstrated that simultaneous reaction and separation can expand the attainable region for single-phase reactors. The procedure allows us to identify reactor and reactor-separator configurations useful in accessing various parts of the feasible region. The method can also be applied to liquid-liquid reactive extraction systems, using models developed recently (Pai et al., 2002).

Acknowledgments

We are grateful to the sponsors of the Process Design and Control Center, University of Massachusetts, Amherst.

Notation

a_i = activity of component i
A, B, C = generic chemical species
c = number of components
F = inlet liquid molar flow rate, mol/s
H = liquid-phase molar holdup
H_j = liquid-phase molar holdup on stage j, mol
$k_{f,k}$ = forward rate constant for the kth reaction, 1/s
L = outlet liquid molar flow rate, mol/s
L_j = liquid molar flow rate from stage j, mol/s
L_j^m = liquid mass flow rate from stage j, kg/s
N = number of two-phase CSTRs in the cascade
R = number of reactions
$\Re$ = reaction rate, mols reacted per mol of reaction per minute
V = vapor flow rate, mol/s
V_j = vapor molar flow rate from stage j, mol/s
V_j^m = vapor mass flow rate from stage j, kg/s
$x_{i,j}$ = mol fraction of component i in the liquid phase for the jth stage
$y_{i,j}$ = mol fraction of component i in the vapor phase for the jth stage
ξ = dimensionless time variable
ρ_j^m = mass density of the liquid phase on stage j
ϕ_j = ratio of vapor rate to the liquid inlet rate for stage j, dimensionless
ϕ_j^m = mass density of the liquid phase on stage j

Literature Cited

Aris, R., "Studies in Optimization: I. The Optimum Design of Adiabatic Reactors with Several Beds," *Chem. Eng. Sci.*, **12**, 243 (1960a).
Aris, R., "Studies in Optimization: II. Optimum Temperature Gradients in Tubular Reactors," *Chem. Eng. Sci.*, **13**, 18 (1960b).
Aris, R., "Studies in Optimization: III. The Optimization Operating Conditions in Sequences of Stirred Tank Reactors," *Chem. Eng. Sci.*, **13**, 75 (1960c).
Aris, R., "Studies in Optimization: IV. The Optimum Conditions for a Single Reaction," *Chem. Eng. Sci.*, **13**, 197 (1961).
Backhaus, A. A., "Continuous Process for the Manufacture of Esters," U. S. Patent No. 1,400,849 (1921a).
Backhaus, A. A., "Apparatus for the Manufacture of Esters," U. S. Patent No. 1,400,850 (1921b).
Backhaus, A. A., "Apparatus for the Production of Esters," U. S. Patent No. 1,400,851 (1921c).
Backhaus, A. A., "Method for the Production of Esters," U. S. Patent No. 1,400,852 (1921d).
Balakrishna, S., and L. T. Biegler, "A Unified Approach for the Simultaneous Synthesis of Reaction, Energy, and Separation Systems," *Ind. Eng. Chem. Res.*, **32**, 1372 (1993).
Buzad, G., and M. F. Doherty, "New Tools for the Design of Kinetically Controlled Reactive Distillation Columns for Ternary Mixtures," *Comp. Chem. Eng.*, **19**, 395 (1995).
Chen, F., R. S. Huss, M. F. Malone, and M. F. Doherty, "Simulation of Kinetic Effects in Reactive Distillation," *Comp. Chem. Eng.*, **24**, 2457 (2000).

Chitra, S. P., and R. Govind, "Yield Optimization for Complex Reactor Systems," *Chem. Eng. Sci.*, **36**, 1219 (1981).
Chitra, S. P., and R. Govind, "Synthesis of Optimal Reactor Structures for Homogeneous Reactions," *AIChE J.*, **31**, 177 (1985).
Damköhler, G., "Strömungs und Wärmeubergangsprobleme in Chemischer Technik and Forschung," *Chem. Ing. Tech.*, **12**, 469 (1939).
Doherty, M. F., and M. F. Malone, *Conceptual Design of Distillation Systems*, McGraw-Hill, New York (2001).
Douglas, J. M., *Conceptual Design of Chemical Processes*, McGraw-Hill, New York (1988).
Feinberg, M., and D. Hildebrandt, "Optimal Reactor Design from a Geometric Viewpoint: I. Universal Properties of the Attainable Region," *Chem. Eng. Sci.*, **52**, 1637 (1997).
Feinberg, M., "Optimal Reactor Design from a Geometric Viewpoint: II. Critical Sidestream Reactors," *Chem. Eng. Sci.*, **55**, 2455 (2000a).
Feinberg, M., "Optimal Reactor Design from a Geometric Viewpoint: III. Critical CFSTRs," *Chem. Eng. Sci.*, **55**, 3553 (2000b).
Feinberg, M., "General Kinetic Bounds on Productivity and Selectivity in Reactor-Separator Systems of Arbitrary Design: Principles," *Ind. Eng. Chem. Res.*, **40**, 3181 (2001).
Gadewar, S. B., "Feasible Products for Reaction with Separation," PhD Diss., Univ. of Massachusetts at Amherst (2002).
Gadewar, S. B., M. F. Malone, and M. F. Doherty, "Selectivity Targets for Batch Reactive Distillation," *Ind. Eng. Chem. Res.*, **39**, 1565 (2000).
Gadewar, S. B., M. F. Doherty, and M. F. Malone, "A Systematic Method for Reaction Invariants and Mole Balances for Complex Chemistries," *Comp. Chem. Eng.*, **25**, 1199 (2001).
Glasser, B., D. Hildebrandt, and D. Glasser, "Optimal Mixing for Exothermic Reversible Reactions," *Ind. Eng. Chem. Res.*, **31**, 1541 (1992).
Glasser, D., D. Hildebrandt, and C. Crowe, "A Geometric Approach to Steady Flow Reactors: The Attainable Region and Optimization in Concentration Space," *Ind. Eng. Chem. Res.*, **26**, 1803 (1987).
Glasser, D., D. Hildebrandt, and S. Godorr, "The Attainable Region for Segregated, Maximum Mixed, and Other Reactor Models," *Ind. Eng. Chem. Res.*, **33**, 1136 (1994).
Godorr, S. A., D. Hildebrandt, and D. Glasser, "The Attainable Region for Systems with Mixing and Multiple-Rate Processes: Finding Optimal Reactor Structures," *Chem. Eng. J.*, **54**, 175 (1994).
Hildebrandt, D., and D. Glasser, "The Attainable Region and Optimal Reactor Structures," *Chem. Eng. Sci.*, **45**, 2161 (1990).
Hildebrandt, D., D. Glasser, and C. Crowe, "Geometry of the Attainable Region Generated by Reaction and Mixing: With and Without Constraints," *Ind. Eng. Chem. Res.*, **29**, 49 (1990).
Holmgren, J. S., D. B. Galloway, L. B. Galperin, and W. R. Willis, "Selective Aromatics Disproportionation/Transalkylation," U. S. Patent No. 6,008,423 (1999).
Horn, F., "Attainable and Non-Attainable Regions in Chemical Reaction Technique," *Euro. Symp. on Chemical Reaction Engineering*, Amsterdam, Pergamon Press, New York, 293 (1964).
Jackson, R., "Optimization of Chemical Reactors with Respect to Flow Configuration," *J. Optim. Theory Appl.*, **2**, 240 (1968).
Keyes, D. B., "Esterification Processes and Equipment," *Ind. Eng. Chem.,* **24**, 1096 (1932).
Kokossis, A. C., and C. A. Floudas, "Optimization of Complex Reactor Networks: I. Isothermal Operation," *Chem. Eng. Sci.*, **45**, 595 (1990).
Kokossis, A. C., and C. A. Floudas, "Optimization of Complex Reactor Networks: II. Nonisothermal Operation," *Chem. Eng. Sci.*, **49**, 1037 (1994).
Lakshmanan, A., and L. T. Biegler, "Synthesis of Optimal Chemical Reactor Networks," *Ind. Eng. Chem. Res.*, **35**, 1344 (1996).
Lee, L.-S., and M.-Z. Kuo, "Phase and Reaction Equilibria of the Acetic Acid–Isopropanol–Isopropyl Acetate–Water System at 760 mm Hg," *Fluid Phase Equilib.*, **123**, 147 (1996).
Levenspiel, O., *Chemical Reaction Engineering*, 2nd ed., Chap. 7, Wiley, New York (1972).
Manning, J. M., "Kinetics and Feasibility of Reactive Distillation in Isopropyl Acetate Synthesis," MS Thesis, University of Massachusetts, Amherst (1999).
Marcoulaki, E. C., and A. C. Kokossis, "Scoping and Screening Complex Reaction Networks using Stochastic Optimization," *AIChE J.*, **45**, 1977 (1999).
Nisoli, A., M. F. Malone, and M. F. Doherty, "Attainable Region for Reaction with Separation," *AIChE J.*, **43**, 374 (1997).
Pahor, B., N. Irsic, and Z. Kravanja, "MINLP Synthesis and Modified Attainable Region Analysis of Reactor Networks in Overall Process Schemes using More Compact Reactor Superstructure," *Comp. Chem. Eng.*, **24**, 1403 (2000).
Pai, R. A., M. F. Doherty, and M. F. Malone, "Design of Reactive Extraction Systems for Bioproduct Recovery," *AIChE J.*, **48**(3), 514 (2002).
Rooney, W. C., B. P. Hausberger, L. T. Biegler, and D. Glasser, "Convex Attainable Region Projections for Reactor Synthesis," *Comp. Chem. Eng.*, **24**, 225 (2000).
Shinnar, R., and C. A. Feng, "Structure of Complex Catalytic Reactions: Thermodynamic Constraints in Kinetic Modeling and Catalyst Evaluation," *Ind. Eng. Chem. Fundam.*, **24**, 153 (1985).
Smith, R. L., and M. F. Malone, "Attainable Region for Polymerization Reaction Systems," *Ind. Eng. Chem. Res.*, **36**, 1076 (1997).
Venimadhavan, G., M. F. Malone, and M. F. Doherty, "Bifurcation Study of Kinetic Effects in Reactive Distillation," *AIChE J.*, **45**, 546 (1999).

Appendix: Dimension of the Feasible Region

The feasible region has the same dimension as the attainable region. The dimension depends on the reaction chemistry and the number of feedstreams, and is given by the degrees of freedom for the overall mol balances over the reaction system. We describe a method based on reaction invariants for determining the dimension of the feasible region.

Consider a reaction system consisting of c components and R independent chemical reactions

$$\nu_{1,r}A_1 + \nu_{2,r}A_2 + \cdots + \nu_{c,r}A_c \rightleftharpoons 0, \qquad r = 1, 2, \ldots, R \quad \text{(A1)}$$

where A_i are the reacting species and $\nu_{i,r}$ is the stoichiometric coefficient of component i in reaction r. The inlet to the reaction system is represented by a vector of inlet molar flow rates of species, $\boldsymbol{n}^0$; the outlet is represented by a vector of outlet flow rates of species $\boldsymbol{n}$. The mol balances for the system are written using reaction invariants which take the same value before, during, and after the reaction (Gadewar et al., 2001). These are

$$N_i^0 = n_i^0 - \boldsymbol{\nu}_i^T(\boldsymbol{\nu}_{\text{ref}})^{-1}\boldsymbol{n}_{\text{Ref}}^0, \qquad i = 1, \ldots, c - R \quad \text{(A2)}$$

$$N_i = n_i - \boldsymbol{\nu}_i^T(\boldsymbol{\nu}_{\text{Ref}})^{-1}\boldsymbol{n}_{\text{Ref}}, \qquad i = 1, \ldots, c - R \quad \text{(A3)}$$

where n_i^0 is the number of mols of component i at the inlet, n_i is the number of mols of component i at the outlet, $\boldsymbol{\nu}_i^T$ is the row vector of dimension R of the stoichiometric coefficients of component i in all of the R reactions. N_i^0 are the reaction invariants based on the inlet molar flow rates, and N_i are the reaction invariants based on the outlet molar flow rates. When we equate these reaction invariants, the mol balances for the reacting system are simply

$$N_i^0 = N_i, \qquad i = 1, \ldots, c - R \quad \text{(A4)}$$

Therefore, the number of mol balances for R independent reactions is $c - R$. The total number of variables for the system is $2c$; therefore, there are $c + R$ degrees of freedom for the reaction system. For a single feedstream of known flow rate and composition, c degrees of freedom are satisfied. Therefore, the dimension of the feasible region is R, which

also is the number of independent chemical reactions. A feasible region together with the mol balances (Eq. A4) and known feed will completely determine the outlet flow rates of all species leaving the reaction system.

Feinberg (2000a) arrives at the same result for the dimension of the attainable region by an alternate method. In general, for multiple distinct feedstreams of known flow rates and compositions, the dimension of the feasible region is determined from the rank of the matrix formed by the reaction stoichiometry matrix augmented by the row vectors for the feedstreams (Feinberg, 2000a). For example, if vectors f_1 and f_2 represent two distinct feeds, the dimension of the feasible region is equal to the rank of the matrix given by the stoichiometric coefficient matrix augmented by a row vector $f_2 - f_1$.

Manuscript received Feb. 12, 2001, and revision received Sept. 21, 2001.